AMERICAN SOCIETY FOR MICROBIOLOGY | Applied and Environmental Microbiology®

GENETICS AND MOLECULAR BIOLOGY

Physical and Functional Interplay between $MazF_1^{Bif}$ and Its Noncognate Antitoxins from *Bifidobacterium longum*

Yanxia Wei,[a] Yang Li,[a,b] Fan Yang,[a] Qiong Wu,[a] Dianbin Liu,[a] Xiangyang Li,[a] Hui Hua,[a] Xiaomei Liu,[a] Yugang Wang,[a] Kuiyang Zheng,[a] Renxian Tang[a]

Department of Pathogenic Biology and Immunology, Jiangsu Key Laboratory of Immunity and Metabolism, Xuzhou Medical University, Xuzhou, China[a]; Jiangsu Vocational College of Nursing, Huaian, China[b]

ABSTRACT *Bifidobacterium longum* strain JDM301, a widely used commercial strain in China, encodes at least two MazEF-like modules and one RelBE-like toxin-antitoxin (TA) system in its chromosome, designated $MazE_1F_1^{Bif}$, $MazE_2F_2^{Bif}$, and $RelBE^{Bif}$, respectively. Bacterial TA systems play an important role in several stress responses, but the relationship between these TA systems is largely unknown. In this study, the interactions between $MazF_1^{Bif}$ and $MazE_2^{Bif}$ or $RelB^{Bif}$ were assessed in *B. longum* strain JDM301. $MazF_1^{Bif}$ caused the degradation of $tufA^{Bif}$ mRNA, and its toxicity was inhibited by forming a protein complex with its cognate antitoxin, $MazE_1^{Bif}$. Notably, $MazF_1^{Bif}$ toxicity was also partially neutralized when jointly expressed with noncognate antitoxin $MazE_2^{Bif}$ or $RelB^{Bif}$. Our results show that the two noncognate antitoxins also inhibited mRNA degradation caused by $MazF_1^{Bif}$ toxin. Furthermore, the physical interplay between $MazF_1^{Bif}$ and its noncognate antitoxins was confirmed by immunoprecipitation. These results suggest that $MazF_1^{Bif}$ can arrest cell growth and that $MazF_1^{Bif}$ toxicity can be neutralized by its cognate and noncognate antitoxins. These results imply that JDM301 uses a sophisticated toxin-antitoxin interaction network to alter its physiology when coping with environmental stress.

IMPORTANCE Although toxin-antitoxin (TA) systems play an important role in several stress responses, the regulatory mechanisms of multiple TA system homologs in the bacterial genome remain largely unclear. In this study, the relationships between $MazE_1F_1^{Bif}$ and the other two TA systems of *Bifidobacterium longum* strain JDM301 were explored, and the interactions between $MazF_1^{Bif}$ and $MazE_2^{Bif}$ or $RelB^{Bif}$ were characterized. In addition, the mRNA degradation activity of $MazF_1^{Bif}$ was demonstrated. In particular, the interaction of the toxin with noncognate antitoxins was shown, even between different TA families ($MazF_1^{Bif}$ toxin and $RelB^{Bif}$ antitoxin) in JDM301. This work provides insight into the regulatory mechanisms of TA systems implicated in the stress responses of bifidobacteria.

KEYWORDS *Bifidobacterium longum*, toxin-antitoxin system, cross-interaction, mRNA degradation

Type II toxin-antitoxin (TA) systems are ubiquitous in free-living bacteria and consist of adjacent genes encoding a toxin and antitoxin in a single operon (1, 2). The first gene encodes a relatively labile antitoxin and the second gene encodes a stable toxin (2). Bacterial TA systems are considered stress-responsive elements (3, 4). Under normal conditions, antitoxin proteins are abundant, which can neutralize the action of its cognate toxin. The toxin and its cognate antitoxin interact to form an inactive toxin-antitoxin protein complex. The complex or the antitoxin itself acts as a transcriptional autorepressor of the operon (5). However, in response to adverse growth conditions, the amount of antitoxin decreases and the toxin is released, leading to cell death or growth arrest by the toxin acting on its intracellular target (5–7). Transcription is

Received 28 November 2016 **Accepted** 9 February 2017

Accepted manuscript posted online 17 February 2017

Citation Wei Y, Li Y, Yang F, Wu Q, Liu D, Li X, Hua H, Liu X, Wang Y, Zheng K, Tang R. 2017. Physical and functional interplay between $MazF_1^{Bif}$ and its noncognate antitoxins from *Bifidobacterium longum*. Appl Environ Microbiol 83:e03232-16. https://doi.org/10.1128/AEM.03232-16.

Editor Christopher A. Elkins, FDA Center for Food Safety and Applied Nutrition

Address correspondence to Kuiyang Zheng, ZKY02@163.com, or Renxian Tang, tangrenxian-t@163.com.

Yanxia Wei and Yang Li contributed equally to this work.

repressed by the antitoxin alone or the toxin-antitoxin complex upon binding to the palindrome upstream of the operon (8). The antitoxin protein is unstable relative to the toxin, since it is susceptible to cleavage by ClpP or/and Lon proteases (9, 10). When stress conditions lead to an increased expression of proteases, the pool of antitoxins is reduced by proteolysis, leading to a relative increase in module transcription, which results in an excess of toxin (5). The free toxin then acts on its target, resulting in transient growth arrest or cell death if antitoxin synthesis does not recover quickly enough (5, 11, 12).

Some TA systems in *Escherichia coli* are activated under environmental stress, resulting in cell stasis, after which they can recover under favorable conditions (13, 14). The MazEF module (toxin MazF and antitoxin MazE) is a well-characterized TA system of *E. coli* that is involved in various stress conditions, such as nutritional stress and antibiotic exposure (15–17). Stress conditions lead to the degradation of the antitoxin (MazE) and the release of the free toxin (MazF). The free MazF prevents translation by cleaving RNAs, resulting in cell death or growth arrest (18–20). The RelBE module (toxin RelE and antitoxin RelB) is another TA system in *E. coli*. Free RelE can induce global inhibition of translation and the arrest of cell growth by cleaving RNAs (21–23). Among them, the *tufA* (elongation factor Tu) mRNAs are targets of free RelE and HigB (toxin protein of the TA system HigBA) in *E. coli* (22–24).

Although TA systems are distributed widely in free-living bacteria, which can encode more than one TA system, almost all intracellular bacteria are devoid of TA systems, suggesting that these systems are stress-response elements, which are crucial for bacterial survival in fluctuating environmental conditions (16, 25–27). However, genomes of free-living bacteria usually encode many TA system homologs (28, 29). The relationships between these TA systems in the bacterial genome are largely unknown. Recently, multiple toxin-antitoxin systems were reported to cooperate to increase the persister frequency in *E. coli* (14). Interactions were also found among three RelB-like TA systems and even between different TA families (MazF toxins and VapB antitoxins) in *Mycobacterium tuberculosis* (30, 31). Nineteen genes of TA systems belonging to the MazEF and RelBE families were found by an *in silico* analysis of 36 sequenced genomes from several strains of bifidobacteria (32). The whole genome of *Bifidobacterium longum* strain JDM301, a widely used commercial strain in China, was completely sequenced (33). A total of 11 putative TA systems were found by bioinformatic analysis of the JDM301 genome (10). The JDM301 genome harbors at least two pairs of functional *mazEF*-like loci (BLJ_811-BLJ_812 and BLJ_864-BLJ_865) and one pair of functional *relBE*-like loci (BLJ_989-BLJ_990), designated $MazE_1F_1^{Bif}$, $MazE_2F_2^{Bif}$, and $RelBE^{Bif}$, respectively (10, 34, 35). In our previous report, we showed that $MazE_1F_1^{Bif}$ was activated under acid stress (10). However, the roles of these systems in the stress response of JDM301 remain largely unclear. The relationships between $MazE_1F_1^{Bif}$ and the other two TA systems were explored in this study.

In this study, the physical and functional interplay between toxin $MazF_1^{Bif}$ and its noncognate antitoxins was characterized. In addition, the mRNA degradation activity of $MazF_1^{Bif}$ was shown. In particular, noncognate interactions were found, even between different TA families ($MazF_1^{Bif}$ toxin and $RelB^{Bif}$ antitoxin) in *B. longum*. Interactions with noncognate antitoxins might reduce the toxicity of $MazF_1^{Bif}$ *in vivo*. This work provides insight on the interplay between different TA systems in *B. longum*, which helps the bacterium adapt to harsh environmental conditions.

RESULTS

$MazF_1^{Bif}$ and its cognate antitoxin, $MazE_1^{Bif}$, form a complex. To show the direct interaction between $MazE_1^{Bif}$ and $MazF_1^{Bif}$, the $MazE_1^{Bif}$ and $MazF_1^{Bif}$ genes were both cloned into a single pET28a expression vector under one promoter in accordance with our previous report (10). Thus, only $MazE_1^{Bif}$ was expressed as a His_6-tagged fusion protein, while $MazF_1^{Bif}$ was expressed as a Myc-tagged fusion protein. The recombinant proteins were expressed and purified from Ni-nitrilotriacetic acid (Ni-NTA) resin. The purified proteins were subjected to Western blot analysis using anti-His_6 or anti-Myc

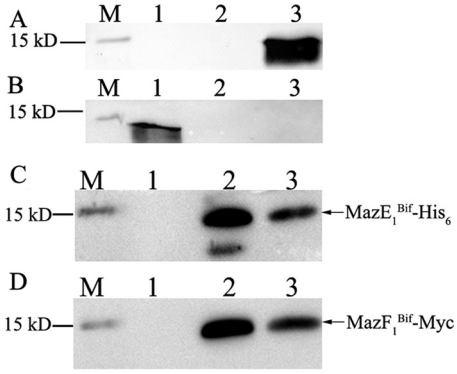

FIG 1 Interaction of Myc-tagged $MazF_1^{Bif}$ and His_6-tagged $MazE_1^{Bif}$ recombinant proteins. Recombinant proteins were expressed and purified using Ni-NTA resin. The purified proteins were detected by Western blotting with anti-His_6 (A) and anti-Myc (B) monoclonal antibodies. Recombinant proteins were expressed from IPTG-induced *E. coli* harboring pET-E_1 or pET-F_1(Myc). M, molecular mass markers; 1, lysate of *E. coli* harboring pET-F_1(Myc); 2, purified products of *E. coli* harboring pET-F_1(Myc); 3, purified recombinant proteins from *E. coli* harboring pET-E_1. (C) $MazE_1^{Bif}$-His_6, including the His_6 tag at its N-terminal end. (D) $MazF_1^{Bif}$-Myc, including the Myc tag at its C-terminal end. Recombinant proteins were expressed from IPTG-induced *E. coli* harboring pET-E_1F_1(Myc). Both the $MazE_1^{Bif}$-His_6 and $MazF_1^{Bif}$-Myc fusion proteins were detected at their expected molecular masses. M, molecular mass markers; 1, eluates of absorbed lysate from uninduced *E. coli* harboring pET-E_1F_1(Myc); 2, eluates of absorbed lysate from IPTG-induced *E. coli* harboring pET-E_1F_1(Myc); 3, purified recombinant proteins from IPTG-induced *E. coli* harboring pET-E_1F_1(Myc).

monoclonal antibodies. The resulting bands observed corresponded to $MazE_1^{Bif}$ (12.6 kDa) with the His_6 tag and to $MazF_1^{Bif}$ (14.4 kDa) with the Myc tag (Fig. 1). Thus, His_6-$MazE_1^{Bif}$ and $MazF_1^{Bif}$-Myc were copurified from Ni^{2+}-chelating Sepharose resin to show that $MazF_1^{Bif}$ and its cognate antitoxin, $MazE_1^{Bif}$, formed a complex.

mRNA degradation by $MazF_1^{Bif}$ is antagonized by its cognate antitoxin, $MazE_1^{Bif}$. The *tufA*^{Bif} gene was cloned into the promoter of the arabinose operon of pBAD/HisB to produce *tufA*^{Bif} mRNA in *E. coli*. pACYCDuet-1, pAD-F_1, or pAD-F_1E_1 was transformed into *E. coli* with pBA-tufA for the coexpression of $MazF_1^{Bif}$ or $MazF_1^{Bif}$ and $MazE_1^{Bif}$ with *tufA*^{Bif} mRNA. Quantitative real-time PCR (qRT-PCR) was used to determine whether $MazF_1^{Bif}$ mediates *tufA* mRNA degradation in strain JDM301 and whether the activity of $MazF_1^{Bif}$ is inhibited by $MazE_1^{Bif}$. Our results show that the induction of $MazF_1^{Bif}$ in *E. coli* decreased *tufA*^{Bif} mRNA levels compared with levels when *tufA*^{Bif} was transcribed alone, while *tufA*^{Bif} mRNA levels increased when $MazF_1^{Bif}$ was coexpressed with $MazE_1^{Bif}$ compared with levels in *E. coli* expressing only $MazF_1^{Bif}$, indicating that $MazE_1^{Bif}$ alleviates the degradation of *tufA*^{Bif} mRNA by MazF^{Bif} (Fig. 2). These results

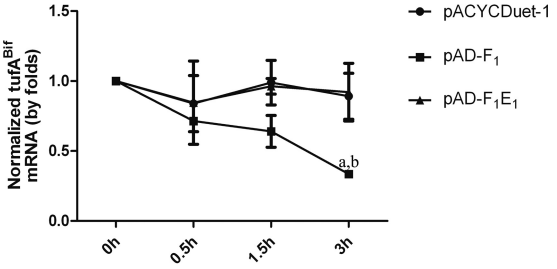

FIG 2 $MazF_1^{Bif}$ is an mRNA interferase that is inhibited by its cognate antitoxin, $MazE_1^{Bif}$. Relative transcript levels of *tufA*^{Bif} were determined in *E. coli* expressing *tufA*^{Bif} with pACYCDuet-1, pAD-F_1, or pAD-F_1E_1. The strains were grown with 0.2% arabinose for 2 h to induce *tufA*^{Bif} expression. Then, 1 mM IPTG was added to induce $MazF_1^{Bif}$ or $MazF_1^{Bif}$ and $MazE_1^{Bif}$ expression. After 3 h, 200 μg/ml rifampin was added. Samples were collected at the indicated time points after rifampin addition. The levels of *tufA*^{Bif} mRNA were monitored by qRT-PCR (normalized to the 16S rRNA transcript level). The values presented are the averages from three independent experiments, and error bars represent the standard deviations. A two-way analysis of variance with Bonferroni posttest was used to obtain *P* values for each time point: a, $P < 0.05$ versus pACYCDuet-1; b, $P < 0.05$ versus pAD-F_1E_1.

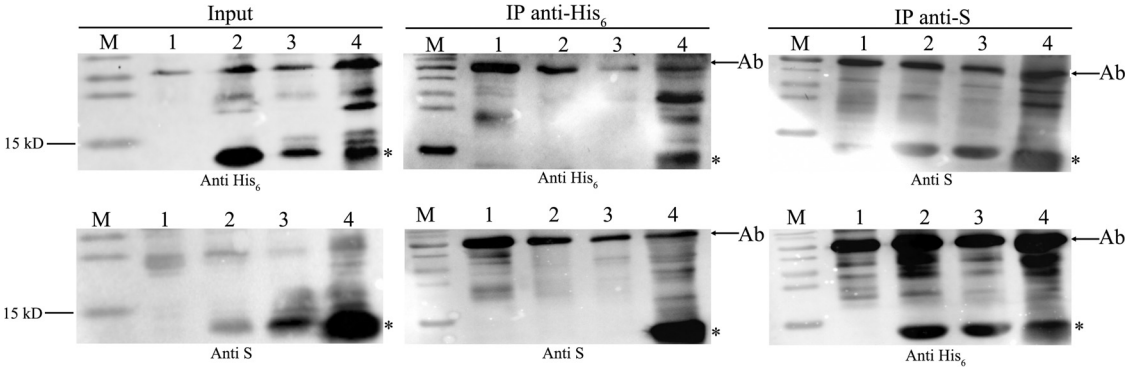

FIG 3 Molecular interactions between $MazF_1^{Bif}$ and cognate or noncognate antitoxin proteins are confirmed by coimmunoprecipitation assays. Cell lysates or proteins immunoprecipitated with the anti-His_6 or anti-S antibodies were analyzed by immunoblotting using anti-His_6 or anti-S antibodies. M, molecular mass markers; 1, *E. coli* carrying pACYCDuet-1 (an empty vector) used as the control; 2, *E. coli* carrying pAD-F_1E_1; 3, *E. coli* carrying pAD-F_1E_2; 4, *E. coli* carrying pAD-F_1B. Asterisks indicate the bands corresponding to $MazF_1^{Bif}$-His_6, $MazE_1^{Bif}$-S, $MazE_2^{Bif}$-S, or $RelB^{Bif}$-S. The bands corresponding to the heavy chains of the anti-His_6 or anti-S antibody are indicated by arrows.

suggest that $MazF_1^{Bif}$ causes the degradation of $tufA^{Bif}$ mRNA and that the activity of $MazF_1^{Bif}$ is alleviated by its cognate, $MazE_1^{Bif}$.

$MazF_1^{Bif}$ physically interacts with its noncognate antitoxin protein. Plasmid pACYCDuet-1, pAD-F_1E_1, pAD-F_1E_2, or pAD-F_1B was introduced into *E. coli* to simultaneously express His-tagged $MazF_1^{Bif}$ and S-tagged antitoxins ($MazE_1^{Bif}$, $MazE_2^{Bif}$, or $RelB^{Bif}$). Subsequently, coimmunoprecipitation was performed to detect the physical interactions between the toxin $MazF_1^{Bif}$ and each of the three antitoxin proteins, including its cognate antitoxin, $MazE_1^{Bif}$, and noncognate antitoxins $MazE_2^{Bif}$ and $RelB^{Bif}$. An anti-His antibody against the His-tagged $MazF_1^{Bif}$ and an anti-S antibody against the S-tagged antitoxins were used in coimmunoprecipitation experiments. As shown in Fig. 3, noncognate toxin-antitoxin interactions ($MazF_1^{Bif}$ with $MazE_2^{Bif}$ and $MazF_1^{Bif}$ with $RelB^{Bif}$) and a cognate toxin-antitoxin interaction ($MazF_1^{Bif}$ with $MazE_1^{Bif}$) were observed by immunoprecipitation. The interaction between the toxin $MazF_1^{Bif}$ and the antitoxin $MazE_2^{Bif}$ was only observed by immunoprecipitation using the anti-S antibody. The interaction between the toxin $MazF_1^{Bif}$ and the antitoxin $MazE_1^{Bif}$ was also confirmed by immunoprecipitation using only the anti-S antibody. The reason for this is unclear; however, steric hindrance stemming from the presence of the His tag might be responsible (30). Our results demonstrated that toxin $MazF_1^{Bif}$ and its noncognate antitoxins physically interact with each other, indicating that the noncognate antitoxins of $MazF_1^{Bif}$, particularly $RelB^{Bif}$, may act in lieu of its cognate antitoxin, $MazE_1^{Bif}$, to inhibit toxicity.

$MazF_1^{Bif}$ inhibits the growth of *E. coli*, and the inhibition is alleviated by its noncognate antitoxin proteins. Several growth curves of *E. coli* strains carrying pACYCDuet-1, pAD-F_1, pAD-F_1E_1, pAD-F_1E_2, or pAD-F_1B in the presence of 1 mM IPTG (isopropyl-β-D-thiogalactopyranoside) were plotted to determine whether the toxicity of the $MazF_1^{Bif}$ toxin could be inhibited by noncognate antitoxins *in vivo*. For *E. coli* strains containing $mazF_1^{Bif}$ alone, growth inhibition was observed upon IPTG induction compared with that of the cells containing an empty vector (Fig. 4A). Furthermore, the cells coexpressing $MazE_1^{Bif}$ and $MazF_1^{Bif}$ grew better than those expressing $MazF_1^{Bif}$ alone but worse than those containing the empty vector (Fig. 4A). Notably, when the $MazF_1^{Bif}$ toxin was induced in the presence of noncognate antitoxin $MazE_2^{Bif}$ or $RelE^{Bif}$, growth inhibition was alleviated (Fig. 4B and C), indicating that cell growth inhibition caused by $MazF_1^{Bif}$ can be rescued by the activity of the noncognate antitoxin $MazE_2^{Bif}$ or $RelE^{Bif}$. These rescue experiments enabled the detection of interactions that may be less stable *in vitro*. Our results demonstrated interactions between $MazF_1^{Bif}$ and noncognate antitoxins $RelE^{Bif}$ and $MazE_2^{Bif}$, which act in lieu of $MazE_1^{Bif}$ to inhibit the activity of $MazF_1^{Bif}$.

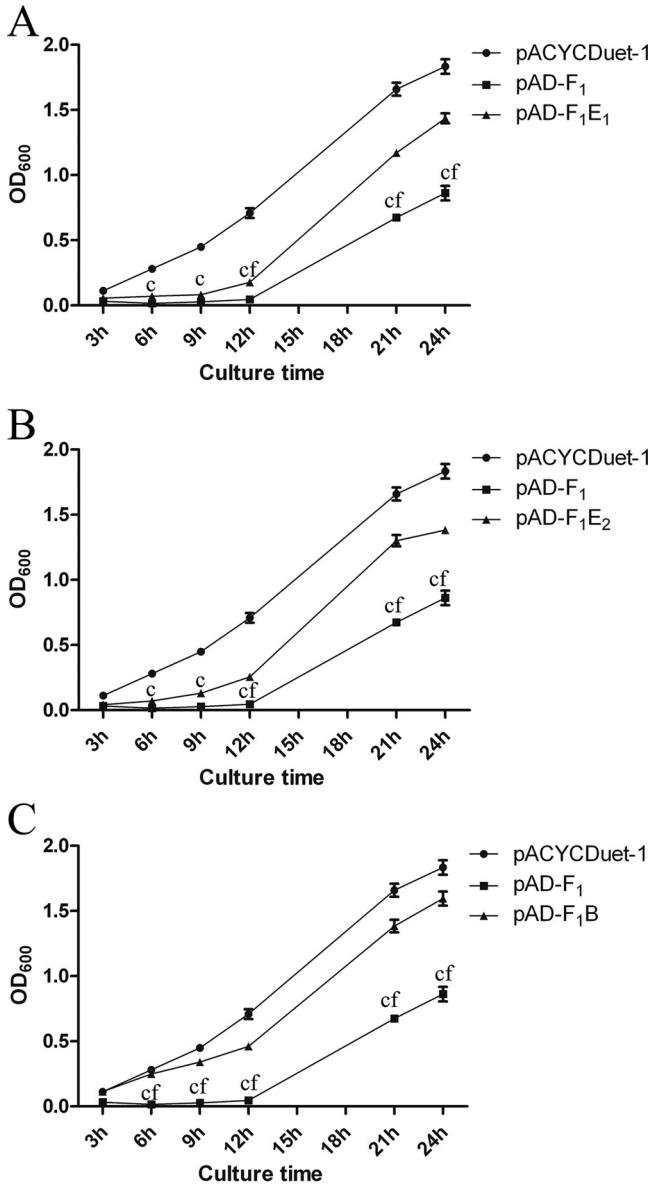

FIG 4 Interactions between $MazF_1^{Bif}$ and its cognate antitoxin, $MazE_1^{Bif}$, or noncognate antitoxins affect cell growth. The growth characteristics of *E. coli* carrying pACYCDuet-1, pAD-F_1, and pAD-F_1E_1 (A), pAD-F_1E_2 (B), or pAD-F_1B (C) were analyzed by measuring absorbance (OD_{600}) following induction with 1 mM IPTG. The values presented are the averages from three independent experiments, and error bars represent the standard deviations. A two-way analysis of variance with Bonferroni posttest was used to obtain *P* values for each time point: c, $P < 0.001$ versus pACYCDuet-1; f, $P < 0.001$ versus pAD-F_1E_1, pAD-F_1E_2, or pAD-F_1B.

$MazF_1^{Bif}$-induced mRNA degradation is antagonized by noncognate antitoxins. The results above showed that the $MazF_1^{Bif}$ toxin associates with the noncognate antitoxin $RelE^{Bif}$ or $MazE_2^{Bif}$ to alleviate growth inhibition caused by $MazF_1^{Bif}$, implying that the toxic effect of $MazF_1^{Bif}$ can be antagonized by noncognate antitoxins. To test this hypothesis, *E. coli* was transformed with pBA-tufA and pACYCDuet-1 (a blank vector), pBA-tufA and pAD-F_1, pBA-tufA and pADuet-F_1E_2, or pBA-tufA and pAD-F_1B. When $RelB^{Bif}$ or $MazE_2^{Bif}$ was coexpressed with $MazF_1^{Bif}$, the level of $tufA^{Bif}$ mRNA increased in comparison to the level of $tufA^{Bif}$ in *E. coli* expressing $MazF_1^{Bif}$ alone (Fig. 5). Our results suggest that $MazF_1^{Bif}$-induced mRNA degradation is inhibited by the noncognate antitoxins $RelE^{Bif}$ and $MazE_2^{Bif}$.

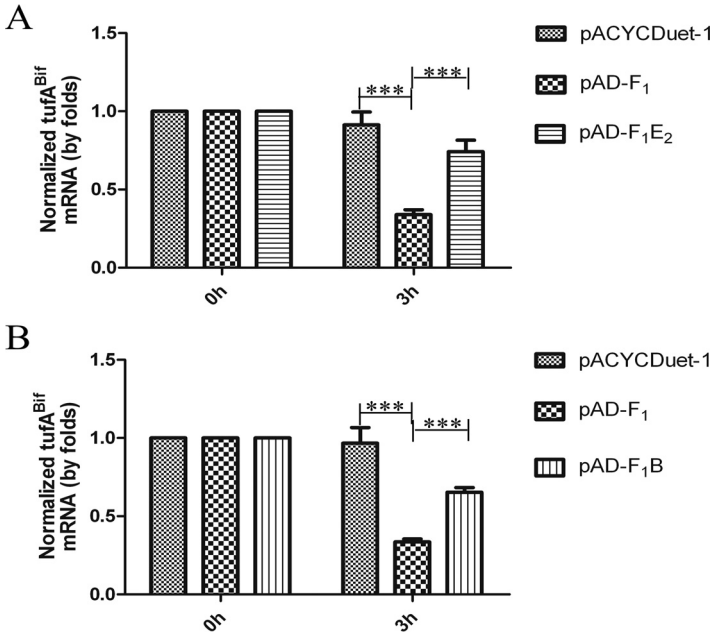

FIG 5 Noncognate antitoxin proteins counteract the mRNA interferase activity of $MazF_1^{Bif}$. Relative transcript levels of *tufA*^{Bif} were determined in *E. coli* expressing *tufA*^{Bif} with pACYCDuet-1, pAD-F_1, and pAD-F_1E_2 (A) or pAD-F_1B (B). The strains were grown with 0.2% arabinose for 2 h to induce *tufA*^{Bif} expression. Then, 1 mM IPTG was added to induce $MazF_1^{Bif}$, $MazF_1^{Bif}$ and $MazE_2^{Bif}$, or $MazF_1^{Bif}$ and RelB^{Bif} expression. After 3 h, 200 μg/ml rifampin was added. Samples were collected at the indicated time points after rifampin addition and the levels of *tufA*^{Bif} mRNA were monitored by qRT-PCR (normalized to the 16S rRNA transcript level). The values presented are the averages from three independent experiments, and error bars represent the standard deviations. A two-way analysis of variance with Bonferroni posttest was used to obtain *P* values for each time point. ***, $P < 0.001$.

DISCUSSION

The cognate toxin and antitoxin of a TA system are small proteins encoded by two genes organized in one operon (36). The activity of the toxin can be neutralized by forming a protein complex with its cognate antitoxin (30, 37). Our results confirmed that the *mazF* homologue (BLJ_811) present in the chromosome of the JDM301 strain encodes a toxic protein ($MazF_1^{Bif}$), which forms a complex with its cognate antitoxin, encoded by the adjacent *mazE* gene (BLJ_812) (10).

To date, toxins of TA systems include ribonucleases, DNA gyrase poisons, phosphotransferases, and protein kinases (2, 38). MazF has been shown to act by cleaving mRNA, resulting in translation inhibition in *E. coli*, *Mycobacterium tuberculosis*, *Streptococcus mutans*, and *Clostridium difficile* (18, 39–41). Like other toxin proteins from *E. coli*, *M. tuberculosis*, *Streptococcus mutans*, and *Clostridium difficile*, the $MazF_1^{Bif}$ toxin was determined to cause mRNA degradation. Our results suggest that $MazF_1^{Bif}$ induces the degradation of *tufA*^{Bif} mRNA, which may partially account for the inhibition of protein synthesis and cell growth arrest. Cleavage of elongation factor Tu mRNAs is partly responsible for growth inhibition caused by $MazF_1^{Bif}$. The $MazF_1^{Bif}$ toxin was not purified in this study because of its low production level in *E. coli*. Thus, we performed an *in vivo* RNase assay with *tufA*^{Bif} mRNAs as the substrate. In previous reports, the homologs of *tufA*^{Bif} were used to determine the RNase activity of RelE and HigB in *E. coli* (23, 24). Our previous work showed that $MazE_1F_1^{Bif}$ is activated through the hydrolysis of $MazE_1^{Bif}$ (10). Therefore, it was proposed that in response to adverse conditions, the antitoxin $MazE_1^{Bif}$ is degraded, releasing the toxin $MazF_1^{Bif}$ to cleave existing transcripts, such as *tufA*^{Bif} mRNA. Consequently, cell growth is modulated and stasis may occur, which may help the cells cope with environmental stress (7).

To date, few studies presenting the interaction between different TA modules have been reported. Yang et al. observed that three *M. tuberculosis* RelE toxins physically interact with the same RelB protein to conditionally regulate RelB binding with pro-

moter DNA (31). Zhu et al. observed noncognate toxin-antitoxin associations, even among different TA families (MazF toxins and VapB antitoxins), in *M. tuberculosis* (30). Recently, transcriptional cross-activation between toxin-antitoxin systems was found in *E. coli* (42). Multiple TA systems have been shown to coordinately govern the persister phenotype in *E. coli* (14). In this study, $MazF_1^{Bif}$ was shown to physically interact with the noncognate antitoxin $RelE^{Bif}$, which belongs to another family of TA systems, or to $MazE_2^{Bif}$ in strain JDM301. Furthermore, when either antitoxin $RelE^{Bif}$ or $MazE_2^{Bif}$ was overexpressed in *E. coli*, cell growth inhibition conferred by the $MazF_1^{Bif}$ toxin was alleviated. Thus, the interaction between $MazE_1F_1^{Bif}$ and $RelBE^{Bif}$ or $MazE_2F_2^{Bif}$ was demonstrated. In addition, $RelE^{Bif}$ and $MazE_2^{Bif}$ antitoxins were observed to antagonize the degradation of $tufA^{Bif}$ mRNA by $MazF_1^{Bif}$. Interestingly, the TA system $MazE_1F_1^{Bif}$ is activated under acid stress (10). In addition, the expression levels of $ClpP_1^{Bif}$ and $ClpP_2^{Bif}$ proteases responsible for the activation of $MazE_1F_1^{Bif}$ are also increased significantly during acid stress (10), whereas $MazE_2F_2^{Bif}$ (data not shown) and $RelBE^{Bif}$ are not activated under this adverse condition (35). As a major challenge to bifidobacteria, acid stress might reduce the viability and probiotic effects of these bacteria (43). TA systems have been implicated in the acid stress response of *E. coli* and *Streptococcus* mutants. In *E. coli*, the antitoxin MqsA mediates the general stress response in bacteria, including the acid stress response (27). Furthermore, a mutated strain of *Streptococcus* devoid of TA systems was shown to be more resistant to changes in pH than the wild-type strain (44).

Generally, there is an excess of antitoxin proteins, since the level of gene expression is often proportional to the gene order in a polycistronic message (i.e., the gene encoding the antitoxin precedes the gene encoding the toxin in the TA operon) (45, 46). In other words, when TA systems are inactivated, the antitoxin proteins exist in excess relative to their cognate toxins (47). Thus, it was speculated that there is an excess of antitoxins ($MazE_2^{Bif}$ and $RelB^{Bif}$) in *B. longum* strain JDM301 under acid stress when TA systems $MazEF_2^{Bif}$ and $RelBE^{Bif}$ are all inactivated. When strain JDM301 was subjected to acid stress, the activation of $MazE_1F_1^{Bif}$ led to the release of free $MazF_1^{Bif}$ toxin resulting in cell growth inhibition. It is possible that excess noncognate antitoxins $MazE_2^{Bif}$ and $RelB^{Bif}$ partially abolish the toxicity of $MazF_1^{Bif}$, helping cells to switch more quickly from a state of growth inhibition to one of normal growth when the acid stress is removed. As a common probiotic bacterium, bifidobacteria are added to many types of fermented dairy foods. However, during the industrial process, storage, and passage through the digestive tract of the host, bifidobacteria are subjected to various stresses, such as acid stress. It was implied that the interaction between $MazF_1^{Bif}$ and $MazE_2^{Bif}$ or $RelB^{Bif}$ may facilitate bacterial adaptation to changing environments encountered during the industrial manufacturing process and passage through the digestive tract of the host. However, the industrial environment is probably not an evolutionary driver of TA systems. TA systems in closely related bifidobacterial species show extensive 95% to 100% similarity, which suggests that horizontal gene transport may account for significant portions of the distribution of TA systems among bifidobacteria (45, 48). Given that the gastrointestinal tract (GIT) is a natural environment of *Bifidobacterium* and a broad variety of bacterial species inhabit the GIT, the main site of horizontal gene transport of bifidobacterial TA modules is the GIT (49, 50). Thus, the harsh conditions in the GIT are the main evolutionary driver of bifidobacterial TA systems. Previously, it was shown that MazEF and RelBE are widely distributed in bifidobacteria (32). Interestingly, among the species, only strain JDM301 and ATCC 15697 have as many TA system genes, while the other bifidobacteria harbor only a few TA systems (48). It was speculated that multiple TA systems may help bifidobacteria to cope with various environmental stresses.

Given that the codon bias and GC content of *B. longum* and *E. coli* are different and that chromosomally encoded $MazF_1^{Bif}$ and antitoxin proteins are heterologously produced by the double promoter plasmid, the heterologous expression of toxin and antitoxin proteins may be influenced. Similarly, in our previous reports, $MazE_1^{Bif}$ did not thoroughly abolish the toxicity of $MazF_1^{Bif}$ when $MazE_1^{Bif}$ and $MazF_1^{Bif}$ were jointly expressed under the control of one promoter, while $MazE_2^{Bif}$ and $RelE^{Bif}$ completely

TABLE 1 Strains and plasmids used in this study

Strain or plasmid	Description	Source or reference
E. coli BL21(DE3)	General expression strain	Tiangen Biotech
B. longum JDM301	Commercial strain	33
pET28a	Expression vector with strong T7 promoter, His tag	Novagen (USA)
pET-E_1	pET28a derivative carrying the $mazE_1^{Bif}$ gene, His tag	This study
pET-F_1(Myc)	pET28a derivative carrying the $mazE_1F_1^{Bif}$ gene, Myc tag	This study
pET-E_1F_1(Myc)	pET28a derivative carrying the $mazE_1F_1^{Bif}$ gene, His tag and Myc tag	10
pBAD/HisB	Expression vector with P_{BAD} promoter, His tag	Invitrogen
pBAD-tufA	pBAD/HisB derivative carrying the $tufA^{Bif}$ gene, His tag	This study
pACYCDuet-1	Expression vector for coexpressing two target genes with T7 promoter, His tag and S tag	Novagen
pAD-F_1	pACYCDuet-1 derivative carrying the $mazF_1^{Bif}$ gene	This study
pAD-F_1E_1	pACYCDuet-1 derivative carrying the $mazF_1^{Bif}$ gene and $mazE_1^{Bif}$ gene	This study
pAD-F_1E_2	pACYCDuet-1 derivative carrying the $mazF_1^{Bif}$ gene and $mazE_2^{Bif}$ gene	This study
pAD-F_1B	pACYCDuet-1 derivative carrying the $relB^{Bif}$ gene and $mazF_1^{Bif}$ gene	This study

neutralized their cognate toxins $MazF_2^{Bif}$ and $RelE^{Bif}$, respectively (10, 34, 35). We speculate that in the original host, $MazF_1^{Bif}$ is inhibited by the compensatory actions of noncognate antitoxins under normal conditions, as $MazE_1^{Bif}$ did not completely abolish the toxicity of $MazF_1^{Bif}$. On the other hand, apart from a species-specific pattern in codon usage, there are also considerable differences among genes in many species (51). Our results may be due to a larger deviation in codon bias between *B. longum* and *E. coli*, leading to a disproportionately lower translation efficiency of $MazE_1^{Bif}$ than of $MazF_1^{Bif}$. Further studies are needed to gain a deeper insight into the role of interactions among TA system families in regulating *B. longum* cell growth. Overall, these results provide molecular insight regarding the interactions of TA systems implicated in the bifidobacterial stress response and can serve as a foundation for future studies of TA systems in their natural host, *B. longum*.

MATERIALS AND METHODS

Bacterial strains and culture conditions. A summary of the bacterial strains used in this study is shown in Table 1. JDM301 was cultured anaerobically in MRS (Difco) supplemented with 0.05% (wt/vol) L-cysteine-HCl at 37°C for 14 to 16 h. The DH5α and BL21(DE3) strains of *E. coli* were each cultured aerobically in LB medium on a rotary shaker (220 rpm) at 37°C or cultured on LB agar plates. When needed, the culture medium was supplemented with 50 μg/ml kanamycin, 35 μg/ml chloramphenicol, 100 μg/ml ampicillin, or 200 μg/ml rifampin for *E. coli*. IPTG was added at a final concentration of 0.5 mM or 1 mM to induce the expression of toxin and antitoxin proteins in *E. coli*. Additionally, 0.2% (wt/vol) arabinose was added to induce the transcription of $tufA^{Bif}$ mRNA driven by the promoter of the arabinose operon (P_{BAD}).

Construction of plasmids. All plasmids used in this study are listed in Table 1. PCR primers and restriction sites used are shown in Table 2. As previously reported (10), the intact TA locus ($mazE_1F_1^{Bif}$) was amplified and cloned into pET28a to yield pET-E_1F_1(Myc), which encodes an N-terminal His_6-tagged $MazE_1^{Bif}$ and a Myc-tagged $MazF_1^{Bif}$ under the control of one promoter. Thus, the native $mazE^{Bif}$-$mazF^{Bif}$ gene organization was kept intact to coexpress $MazF_1^{Bif}$ and $MazE_1^{Bif}$ under the control of one promoter. The full-length $tufA^{Bif}$ gene was amplified and cloned into pBAD/HisB to yield pBA-tufA (35). The $mazF_1^{Bif}$ gene was placed under the control of the T7 promoter-1 of pACYCDuet-1, to yield pAD-F_1. The $mazE_1^{Bif}$, $mazE_2^{Bif}$, and $relB^{Bif}$ genes were amplified and subcloned under the control of the T7 promoter-2 of pAD-F_1, resulting in pAD-F_1E_1, pAD-F_1E_2, and pAD-F_1B, respectively. All the genes were amplified using JDM301 genomic DNA as the template, which was extracted from mid-log-phase cultures grown in MRS broth.

Assessment of toxin and antitoxin activities in *E. coli*. *E. coli* strains carrying pACYCDuet-1 (a blank vector), pAD-F_1, pAD-F_1E_1, pAD-F_1E_2, or pAD-F_1B were grown in LB broth with IPTG (1 mM) to induce gene expression. Growth curves of the *E. coli* carrying the corresponding vectors were determined by measuring the OD values at 600 nm (OD_{600}) to assess the effects of the toxin and antitoxin on cell growth. Cultures of the *E. coli* strains were initially grown in LB overnight with 35 μg/ml chloramphenicol and then transferred into fresh LB using 1% inoculum in the presence of 1 mM IPTG (IPTG was added to the LB at 0 h). Samples were taken at different time points, and the optical density at 600 nm was determined for each.

***In vivo* cleavage of the $tufA^{Bif}$ mRNA.** pBA-$tufA^{Bif}$ and pACYCDuet-1 (a blank vector), pBA-$tufA^{Bif}$ and pAD-F_1, pBA-tufA and pAD-F_1E_1, pBA-tufA and pAD-F_1E_2, or pBA-tufA and pAD-F_1B were transformed into *E. coli* to determine whether $MazF_1^{Bif}$ causes the degradation of $tufA^{Bif}$ mRNA and whether $MazF_1^{Bif}$ toxicity is inhibited by its cognate antitoxin, $MazE_1^{Bif}$, or noncognate antitoxins $MazE_2^{Bif}$ and $RelB^{Bif}$. The plasmids used are listed in Table 1, and primers for qRT-PCR of $tufA^{Bif}$ mRNA are listed in Table 2. Cells transformed with the corresponding plasmids were grown at 37°C on a rotary shaker. When the cultures

TABLE 2 Oligonucleotide primers used in PCR and qRT-PCR

Gene	Assay	Direction	Primer sequence[a]	Length (bp)	Source or reference
$mazF_1^{Bif}$	PCR	Sense	CCG**GAATTC**AATGAAACGAGGTGAGATT	324	This work
		Antisense	CCC**AAGCTT**TCACAGCAAACCTAGAAC		
$mazF_1^{Bif}$ (primer $mazF_1^{Bif}$-2)	PCR	Sense	TTAAGAAGGAGATATA**CCATGG**AAATGAAACGAGGTGAGATTCG	354	This work
		Antisense	CTCGAGTGCGGCCGC**AAGCTT**TTACAGATCCTCTTCTGAGATGAGTTTTTGTTC CAGCAAACCTAGAACCCG		
$mazE_1^{Bif}$	PCR	Sense	GGA**AGATCT**AATGAGCATACAGATTGCCA	246	This work
		Antisense	CCG**CTCGAG**CCTCGTTTCATCGGACAT		
$mazE_1^{Bif}$ (primer $mazE_1^{Bif}$-2)	PCR	Sense	**GGATCC**ATGAGCATACAGATTGCCA	246	This work
		Antisense	**CTCGAG**CCTCGTTTCATCGGACAT		
$mazE_2^{Bif}$	PCR	Sense	GGA**AGATCT**TATGGCTATCAAGGAGAAGG	294	This work
		Antisense	CCG**CTCGAG**GTCTTCATCATCGTCCCA		
$relB^{Bif}$	PCR	Sense	GGA**AGATCT**ATTGTCTTACGTAATGATGTTGG	300	This work
		Antisense	CCG**CTCGAG**GATTCCCAACGAATCGAA		
$mazE^{Bif}$	qRT-PCR	Sense	GCTGCGTTGTTTAAGGAGAC	94	10
		Antisense	ACCCACGGTAATCATTGAAC		
$tufA^{Bif}$	qRT-PCR	Sense	ATCCGTCCGACCCAGACC	123	54
		Antisense	CTCGACATCCTCACGGCC		
16S	qRT-PCR	Sense	TACGGGAGGCAGCAG	191	55
		Antisense	ATTACCGCGGCTGCTGG		

[a]Restriction sites for XhoI, EcoRI, BglII, and HindIII incorporated into the primers are in boldface, and the sequence for the Myc tag is underlined.

reached an OD_{600} of 0.5, 0.2% L-arabinose was added to the medium to induce the transcription of $tufA^{Bif}$ mRNA. After incubating at 28°C for 2 h, 1 mM IPTG was added to induce the expression of toxin (and antitoxin) proteins for 3 h. Then, 200 μg/ml rifampin was added to halt transcription. At different time points, 2-ml aliquots were taken. qRT-PCR was performed to determine the level of $tufA^{Bif}$ mRNA. The transcription of 16S rRNA genes in *E. coli* was evaluated as an internal control.

Quantitative real-time PCR. Total RNA was extracted from *E. coli* strains carrying pBA-tufA and pACYCDuet-1 (a blank vector), pBA-tufA and pAD-F_1, pBA-tufA and pADuet-F_1E_1, pBA-tufA and pAD-F_1E_2, or pBA-tufA and pAD-F_1B and was treated with DNase (Roche, Basel, Switzerland). For use in qRT-PCR, cDNA was generated from total RNA (2 μg) using a Superscript III first strand synthesis RT-PCR kit (Invitrogen, Carlsbad, California, USA) according to the manufacturer's protocol. Primers targeting $tufA^{Bif}$ were designed for detecting mRNA expression by qRT-PCR. The primers used are shown in Table 2. The reaction was performed with an ABI 7500 system (Applied Biosystems, Branchburg, New Jersey, USA) using the following conditions: 95°C for 10 min, followed by 40 cycles at 95°C for 15 s and 60°C for 1 min. Calculations were performed using the 16S rDNA gene as an internal standard. The $2^{-\Delta\Delta CT}$ method was used to determine the relative gene expression (52).

Protein purification and Western blot analysis. pET-E_1, pET-F_1(Myc), and pET-E_1F_1(Myc) were transferred into *E. coli* to express the His-tagged $MazE_1^{Bif}$ and/or Myc-tagged $MazF_1^{Bif}$ recombinant proteins. Cells transformed with the corresponding plasmids were grown at 37°C on a rotary shaker. When the cultures reached an OD_{600} of 0.5, IPTG (at a final concentration of 0.5 mM) was added to induce the expression of recombinant fusion proteins (His-tagged $MazE_1^{Bif}$ and Myc-tagged $MazF_1^{Bif}$) for 5 h. The cells were pelleted and disrupted on ice by sonication, and the soluble or insoluble fraction was recovered by centrifugation. The recombinant proteins were purified by affinity chromatography using Ni-NTA resin (Qiagen, Hilden, Germany) according to the manufacturer's protocol. The purified proteins were fractionated by 15% SDS-PAGE and transferred to a nitrocellulose membrane for detection by Western blot analysis. Anti-His and anti-Myc monoclonal antibodies were used to detect His-tagged $MazE_1^{Bif}$ and Myc-tagged $MazF_1^{Bif}$, respectively.

Coimmunoprecipitation assay. *E. coli* strains carrying pACYCDuet-1 (a blank vector), pAD-F_1E_1, pAD-F_1E_2, or pAD-F_1B were grown in LB until an OD_{600} of 0.5 was reached. After that, IPTG (at a final concentration of 1 mM) was added to the medium to induce protein expression for 5 h at 28°C. The cells were pelleted, and the proteins were isolated and immunoprecipitated as described previously (53) with a few modifications. Protein extracts (400 μg) were incubated with anti-His (His-probe [G-18], sc-804; Santa Cruz Biotechnology) or anti-S (MB2016; Bioworld Technology) antibodies on a rotator overnight at 4°C. The immunoprecipitated proteins were incubated with protein A/G agarose (P2012; Beyotime Biotechnology) for 4 h at 4°C. The immunoprecipitated complexes were dissolved in 2× SDS gel loading buffer (at a final concentration of 2% [wt/vol] SDS, 0.1% [wt/vol] bromophenol blue, 10% glycerol, and 50 mM Tris/HCl, pH 6.8). Then, the samples were incubated at 95°C for 5 min and subjected to SDS-PAGE. Extracted proteins and immunocomplexes were analyzed by immunoblotting using anti-His or anti-S monoclonal antibodies. A horseradish peroxidase-labeled goat anti-rabbit IgG antibody was used as a secondary antibody (sc-2054; Santa Cruz Biotechnology). Chemiluminescence signals were visualized with an enhanced chemiluminescence (ECL) reagent (Thermo Scientific, Rockford, Illinois, USA) and were exposed to film.

ACKNOWLEDGMENTS

This work was funded by the National Natural Science Foundation of China (31300029), the Natural Science Foundation of Jiangsu Province, China (BK20130213), the Scientific Research Foundation for the Talents of Xuzhou Medical University (D2012014), the Program for Youth Science and Technology Innovative Research Team of Xuzhou Medical University, the Priority Academic Program Development of Jiangsu Higher Education Institutions (PAPD), and the Scientific Research Innovation Project for College Graduates of Jiangsu Province (KYZZ15_0389) and was sponsored by the Qing Lan Project of Jiangsu Province, China.

The funders had no role in the study design, data collection and interpretation, or the decision to submit the work for publication.

REFERENCES

1. Buts LLJ, Dao-Thi MH, Wyns L, Loris R. 2005. Toxin-antitoxin modules as bacterial metabolic stress managers. Trends Biochem Sci 30:672–679. https://doi.org/10.1016/j.tibs.2005.10.004.
2. Van Melderen L, Saavedra De Bast M. 2009. Bacterial toxin-antitoxin systems: more than selfish entities? PLoS Genet 5:e1000437. https://doi.org/10.1371/journal.pgen.1000437.
3. Gerdes K, Christensen SK, Lobner-Olesen A. 2005. Prokaryotic toxin-antitoxin stress response loci. Nat Rev Microbiol 3:371–382. https://doi.org/10.1038/nrmicro1147.
4. Sala A, Calderon V, Bordes P, Genevaux P. 2013. TAC from Mycobacterium tuberculosis: a paradigm for stress-responsive toxin-antitoxin systems controlled by SecB-like chaperones. Cell Stress Chaperones 18:129–135. https://doi.org/10.1007/s12192-012-0396-5.
5. Sofos N, Xu K, Dedic E, Brodersen DE. 2015. Cut to the chase–regulating translation through RNA cleavage. Biochimie 114:10–17. https://doi.org/10.1016/j.biochi.2015.01.009.
6. Ramage HR, Connolly LE, Cox JS. 2009. Comprehensive functional analysis of Mycobacterium tuberculosis toxin-antitoxin systems: implications for pathogenesis, stress responses, and evolution. PLoS Genet 5:e1000767. https://doi.org/10.1371/journal.pgen.1000767.
7. Maisonneuve E, Shakespeare LJ, Jorgensen MG, Gerdes K. 2011. Bacterial persistence by RNA endonucleases. Proc Natl Acad Sci U S A 108:13206–13211. https://doi.org/10.1073/pnas.1100186108.
8. Zorzini V, Buts L, Schrank E, Sterckx YG, Respondek M, Engelberg-Kulka H, Loris R, Zangger K, van Nuland NA. 2015. Escherichia coli antitoxin MazE as transcription factor: insights into MazE-DNA binding. Nucleic Acids Res 43:1241–1256. https://doi.org/10.1093/nar/gku1352.
9. Donegan NP, Thompson ET, Fu Z, Cheung AL. 2010. Proteolytic regulation of toxin-antitoxin systems by ClpPC in Staphylococcus aureus. J Bacteriol 192:1416–1422. https://doi.org/10.1128/JB.00233-09.
10. Wei YX, Ye L, Liu DB, Zhang ZY, Liu C, Guo XK. 2015. Activation of the chromosomally encoded mazEF(Bif) locus of Bifidobacterium longum under acid stress. Int J Food Microbiol 207:16–22. https://doi.org/10.1016/j.ijfoodmicro.2015.04.028.
11. Schifano JM, Woychik NA. 2014. 23S rRNA as an a-Maz-ing new bacterial toxin target. RNA Biol 11:101–105. https://doi.org/10.4161/rna.27949.
12. Amitai S, Yassin Y, Engelberg-Kulka H. 2004. MazF-mediated cell death in Escherichia coli: a point of no return. J Bacteriol 186:8295–8300. https://doi.org/10.1128/JB.186.24.8295-8300.2004.
13. Islam S, Benedik MJ, Wood TK. 2015. Orphan toxin OrtT (YdcX) of Escherichia coli reduces growth during the stringent response. Toxins (Basel) 7:299–321. https://doi.org/10.3390/toxins7020299.
14. Fasani RA, Savageau MA. 2013. Molecular mechanisms of multiple toxin-antitoxin systems are coordinated to govern the persister phenotype. Proc Natl Acad Sci U S A 110:E2528–E2537. https://doi.org/10.1073/pnas.1301023110.
15. Kwan BW, Lord DM, Peti W, Page R, Benedik MJ, Wood TK. 2014. The MqsR/MqsA toxin/antitoxin system protects Escherichia coli during bile acid stress. Environ Microbiol 17:3168–3181. https://doi.org/10.1111/1462-2920.12749.
16. Norton JP, Mulvey MA. 2012. Toxin-antitoxin systems are important for niche-specific colonization and stress resistance of uropathogenic Escherichia coli. PLoS Pathog 8:e1002954. https://doi.org/10.1371/journal.ppat.1002954.
17. Hazan RSB, Engelberg-Kulka H. 2004. Escherichia coli mazEF-mediated cell death is triggered by various stressful conditions. J Bacteriol 186:3663–3669. https://doi.org/10.1128/JB.186.11.3663-3669.2004.
18. Rothenbacher FP, Suzuki M, Hurley JM, Montville TJ, Kirn TJ, Ouyang M, Woychik NA. 2012. Clostridium difficile MazF toxin exhibits selective, not global, mRNA cleavage. J Bacteriol 194:3464–3474. https://doi.org/10.1128/JB.00217-12.
19. Zhang Y, Zhang J, Hoeflich KP, Ikura M, Qing G, Inouye M. 2003. MazF cleaves cellular mRNAs specifically at ACA to block protein synthesis in Escherichia coli. Mol Cell 12:913–923. https://doi.org/10.1016/S1097-2765(03)00402-7.
20. Wang X, Wood TK. 2011. Toxin/antitoxin systems influence biofilm and persister cell formation and the general stress response. Appl Environ Microbiol 77:5577–5583. https://doi.org/10.1128/AEM.05068-11.
21. Cheverton AM, Gollan B, Przydacz M, Wong CT, Mylona A, Hare SA, Helaine S. 2016. A Salmonella toxin promotes persister formation through acetylation of tRNA. Mol Cell 63:86–96. https://doi.org/10.1016/j.molcel.2016.05.002.
22. Christensen SK, Gerdes K. 2003. RelE toxins from bacteria and Archaea cleave mRNAs on translating ribosomes, which are rescued by tmRNA. Mol Microbiol 48:1389–1400. https://doi.org/10.1046/j.1365-2958.2003.03512.x.
23. Hurley JM, Cruz JW, Ouyang M, Woychik NA. 2011. Bacterial toxin RelE mediates frequent codon-independent mRNA cleavage from the 5′ end of coding regions in vivo. J Biol Chem 286:14770–14778. https://doi.org/10.1074/jbc.M110.108969.
24. Hurley JM, Woychik NA. 2009. Bacterial toxin HigB associates with ribosomes and mediates translation-dependent mRNA cleavage at A-rich sites. J Biol Chem 284:18605–18613. https://doi.org/10.1074/jbc.M109.008763.
25. Makarova KS, Wolf YI, Koonin EV. 2009. Comprehensive comparative-genomic analysis of type 2 toxin-antitoxin systems and related mobile stress response systems in prokaryotes. Biol Direct 4:19. https://doi.org/10.1186/1745-6150-4-19.
26. Frampton R, Aggio RB, Villas-Boas SG, Arcus VL, Cook GM. 2012. Toxin-antitoxin systems of Mycobacterium smegmatis are essential for cell survival. J Biol Chem 287:5340–5356. https://doi.org/10.1074/jbc.M111.286856.
27. Wang X, Kim Y, Hong SH, Ma Q, Brown BL, Pu M, Tarone AM, Benedik MJ, Peti W, Page R, Wood TK. 2011. Antitoxin MqsA helps mediate the bacterial general stress response. Nat Chem Biol 7:359–366. https://doi.org/10.1038/nchembio.560.
28. Pandey DP, Gerdes K. 2005. Toxin-antitoxin loci are highly abundant in free-living but lost from host-associated prokaryotes. Nucleic Acids Res 33:966–976. https://doi.org/10.1093/nar/gki201.
29. Fiedoruk K, Daniluk T, Swiecicka I, Sciepuk M, Leszczynska K. 2015. Type II toxin-antitoxin systems are unevenly distributed among Escherichia coli phylogroups. Microbiology 161:158–167. https://doi.org/10.1099/mic.0.082883-0.
30. Zhu LSJ, Kobayashi H, Woychik NA, Inouye M. 2010. Noncognate mycobacterium tuberculosis toxin-antitoxins can physically and functionally interact. J Biol Chem 285:39732–39738. https://doi.org/10.1074/jbc.M110.163105.
31. Yang M, Gao C, Wang Y, Zhang H, He ZG. 2010. Characterization of the interaction and cross-regulation of three Mycobacterium tuberculosis

RelBE modules. PLoS One 5:e10672. https://doi.org/10.1371/journal.pone.0010672.
32. Averina OV, Alekseeva MG, Abilev SK, Il'in VK, Danilenko VN. 2013. Distribution of genes of toxin-antitoxin systems of mazEF and relBE families in bifidobacteria from human intestinal microbiota. Genetika 49:315–327. (*In* Russian.)
33. Wei YX, Zhang ZY, Liu C, Zhu YZ, Zhu YQ, Zheng H, Zhao GP, Wang S, Guo XK. 2010. Complete genome sequence of Bifidobacterium longum JDM301. J Bacteriol 192:4076–4077. https://doi.org/10.1128/JB.00538-10.
34. Wei YX, Ye L, Liu DB, Guo XK. 2014. A type II toxin-antitoxin system encoded by BLJ_864 and BLJ_865 in the chromosome of Bifidobacterium longum. J Shanghai Jiaotong Univ Med Sci 34:1319–1324.
35. Wei YX, Ye L, Li Y, Yang F, Liu DB, Guo XK, Tang RX, Liu C. 2016. Functional characterization of RelBE toxin-antitoxin system in probiotic Bifidobacterium longum JDM301. Acta Biochim Biophys Sin (Shanghai) 48:741–749. https://doi.org/10.1093/abbs/gmw056.
36. Barbosa LC, Garrido SS, Marchetto R. 2015. BtoxDB: a comprehensive database of protein structural data on toxin-antitoxin systems. Comput Biol Med 58:146–153. https://doi.org/10.1016/j.compbiomed.2015.01.010.
37. Lee HJ, Jin HM, Park MS, Park W, Madsen EL, Jeon CO. 2015. Recovery of plasmid pEMB1, whose toxin-antitoxin system stabilizes an ampicillin resistance-conferring β-lactamase gene in Escherichia coli, from natural environments. Appl Environ Microbiol 81:40–47. https://doi.org/10.1128/AEM.02691-14.
38. Kaspy I, Rotem E, Weiss N, Ronin I, Balaban NQ, Glaser G. 2013. HipA-mediated antibiotic persistence via phosphorylation of the glutamyl-tRNA-synthetase. Nat Commun 4:3001. https://doi.org/10.1038/ncomms4001.
39. Tiwari P, Arora G, Singh M, Kidwai S, Narayan OP, Singh R. 2015. MazF ribonucleases promote Mycobacterium tuberculosis drug tolerance and virulence in guinea pigs. Nat Commun 6:6059. https://doi.org/10.1038/ncomms7059.
40. Zhang Y, Zhang J, Hara H, Kato I, Inouye M. 2005. Insights into the mRNA cleavage mechanism by MazF, an mRNA interferase. J Biol Chem 280:3143–3150. https://doi.org/10.1074/jbc.M411811200.
41. Syed MA, Koyanagi S, Sharma E, Jobin MC, Yakunin AF, Levesque CM. 2011. The chromosomally-encoded mazEFSmu locus of Streptococcus mutans encodes a functional type ii toxin-antitoxin addiction system. J Bacteriol 193:1122–1130. https://doi.org/10.1128/JB.01114-10.
42. Kasari V, Mets T, Tenson T, Kaldalu N. 2013. Transcriptional cross-activation between toxin-antitoxin systems of Escherichia coli. BMC Microbiol 13:45. https://doi.org/10.1186/1471-2180-13-45.
43. Jin J, Qin Q, Guo H, Liu S, Ge S, Zhang H, Cui J, Ren F. 2015. Effect of pre-stressing on the acid-stress response in Bifidobacterium revealed using proteomic and physiological approaches. PLoS One 10:e0117702. https://doi.org/10.1371/journal.pone.0117702.
44. Lemos JA, Brown TA, Jr, Abranches J, Burne RA. 2005. Characteristics of Streptococcus mutans strains lacking the MazEF and RelBE toxin-antitoxin modules. FEMS Microbiol Lett 253:251–257. https://doi.org/10.1016/j.femsle.2005.09.045.
45. Leplae R, Geeraerts D, Hallez R, Guglielmini J, Dreze P, Van Melderen L. 2011. Diversity of bacterial type II toxin-antitoxin systems: a comprehensive search and functional analysis of novel families. Nucleic Acids Res 39:5513–5525. https://doi.org/10.1093/nar/gkr131.
46. Yamaguchi Y, Inouye M. 2011. Regulation of growth and death in Escherichia coli by toxin-antitoxin systems. Nat Rev Microbiol 9:779–790. https://doi.org/10.1038/nrmicro2651.
47. Heaton BE, Herrou J, Blackwell AE, Wysocki VH, Crosson S. 2012. Molecular structure and function of the novel BrnT/BrnA toxin-antitoxin system of Brucella abortus. J Biol Chem 287:12098–12110. https://doi.org/10.1074/jbc.M111.332163.
48. Averina O, Alekseeva M, Shkoporov A, Danilenko V. 2015. Functional analysis of the type II toxin-antitoxin systems of the MazEF and RelBE families in Bifidobacterium longum subsp. infantis ATCC 15697. Anaerobe 35:59–67. https://doi.org/10.1016/j.anaerobe.2015.07.007.
49. Huddleston JR. 2014. Horizontal gene transfer in the human gastrointestinal tract: potential spread of antibiotic resistance genes. Infect Drug Resist 7:167–176. https://doi.org/10.2147/IDR.S48820.
50. Hayes F, Van Melderen L. 2011. Toxins-antitoxins: diversity, evolution and function. Crit Rev Biochem Mol Biol 46:386–408. https://doi.org/10.3109/10409238.2011.600437.
51. Sharp PM, Cowe E, Higgins DG, Shields DC, Wolfe KH, Wright F. 1988. Codon usage patterns in Escherichia coli, Bacillus subtilis, Saccharomyces cerevisiae, Schizosaccharomyces pombe, Drosophila melanogaster and Homo sapiens; a review of the considerable within-species diversity. Nucleic Acids Res 16:8207–8211. https://doi.org/10.1093/nar/16.17.8207.
52. Livak KJ, Schmittgen TD. 2001. Analysis of relative gene expression data using real-time quantitative PCR and the 2(-delta delta C[T]) method. Methods 25:402–408. https://doi.org/10.1006/meth.2001.1262.
53. Akache B, MacPherson S, Sylvain MA, Turcotte B. 2004. Complex interplay among regulators of drug resistance genes in Saccharomyces cerevisiae. J Biol Chem 279:27855–27860. https://doi.org/10.1074/jbc.M403487200.
54. Sheu SJ, Hwang WZ, Chiang YC, Lin WH, Chen HC, Tsen HY. 2010. Use of tuf gene-based primers for the PCR detection of probiotic Bifidobacterium species and enumeration of bifidobacteria in fermented milk by cultural and quantitative real-time PCR methods. J Food Sci 75:M521–527. https://doi.org/10.1111/j.1750-3841.2010.01816.x.
55. Zhou Y, Lin P, Li Q, Han L, Zheng H, Wei Y, Cui Z, Ni Y, Guo X. 2010. Analysis of the microbiota of sputum samples from patients with lower respiratory tract infections. Acta Biochim Biophys Sin (Shanghai) 42:754–761. https://doi.org/10.1093/abbs/gmq081.